Surface tension of strange stars mediated by a color-flavor-locked equation of state

Robert S. Bogadi,* Megandhren Govender,† and Sibusiso Moyo‡
Department of Mathematics, Faculty of Applied Sciences, Durban University of Technology, Durban 4000, South Africa

(Received 27 May 2020; revised 7 August 2020; accepted 11 August 2020; published 31 August 2020)

We investigate the surface tension of strange quark stars by making use of a color-flavor-locked (CFL) equation of state. Compact objects with anisotropic pressures provide richer systems for studying surface tension variations, and establishing physically viable ranges of parameters in maintaining hydrostatic equilibrium of quark matter at densities exceeding that of nuclear material. The strange quark mass, the QCD gap energy, and the MIT bag constant are key parameters in the CFL equation of state used, and thus feature in calculations of the surface tension.

DOI: 10.1103/PhysRevD.102.043026

I. INTRODUCTION

Compact objects such as neutron stars and the proposed strange quark stars composed of deconfined u, d, s quark matter (*strange matter*) [1] offer scenarios in which matter exists under the most extreme and exotic conditions. The theory of QCD has been used to study the properties of quark matter in order to ascertain the prospects for the existence of strange stars [2,3], and possible stellar candidates have been identified [4]. One of the outcomes of the study of the microphysics of quark material is the so-called color-flavor-locked (CFL) superconducting phase in which statistical analyses lead to a description in terms of macroscopic properties, typically the pressure and energy density in order to determine an equation of state. The complex nature of such a study, together with the simplifying assumptions made, can benefit from calculations made using the classical theory of general relativity (GR) whereby the bulk properties of the system are gleaned. In addition to determining an equation of state, it is also necessary to consider the stability of such ultracompact quark matter, and the surface tension could play a significant role in addition to calculations of the adiabatic index, which are typically done. It has been shown recently by Sagun *et al.* [5] that an equation of state which incorporates an induced surface tension component significantly lowers pressures and energy densities which can become excessive at high baryon densities. More importantly, they also note that the induced surface tension helps maintain causality, which is not possible for a van der Waals equation of state with baryon densities exceeding $0.4/\mathrm{fm}^3$. In compact stars, the gravitational force on the particles is very large, and the surface tension does not only depend on the interactions within the strange quark matter but also on the structure of the star as a whole [6]. Surface tension estimates have been an outcome of thermodynamic calculations in which quark matter is confined to strangelets typically of the order of a few femtometers in size, though there is no upper bound to the size of such composite particles [7]. Values in the range $\sigma = 5 \sim 30\ \mathrm{MeV/fm}^2$ have been calculated according to the framework of the Dyson-Schwinger equations of QCD [8]. Other models have given larger values, namely $30 \sim 70\ \mathrm{MeV/fm}^2$ from a quasiparticle model [9] and even $145 \sim 165\ \mathrm{MeV/fm}^2$ according to the Nambu–Jona-Lasinio model [10,11]. Thus, there is still uncertainty in calculating the surface tension of strange stars, and the long-range surface structure could also be of importance. In considering the star as a whole, it is useful to generate relationships between surface tension and physical parameters such as the surface tangential pressure and density which can be obtained easily via the field equations of general relativity.

Early work by Bowers and Laing [12] on anisotropic compact objects in general relativity indicated that the role of anisotropy is significant in stellar cores with densities greater than $10^{15}\ \mathrm{g.cm}^{-3}$. The source of local anisotropy can be attributed to the interactions between neutrons which lead to a superfluid state. In addition, properties such as the presence of a solid core, viscosity and exotic phase transitions leading to a pion condensed state, can also influence pressure anisotropy. The role of pressure anisotropy has also been studied extensively by Herrera *et al.* [13,14].

Since the Einstein field equations of general relativity have the reputation for offering physically nonviable solutions as shown by Delgaty and Lake [15], it is of

*bogadi.robert@gmail.com
†megandhreng@dut.ac.za
‡moyos@dut.ac.za

interest to assert the validity of solutions obtained from GR by considering the incorporation of additional phenomena such as electromagnetic fields [16]. Specific to our study, we include the quark parameters which define both the microstructure and through suitable statistics also the macroscopic state functions. This adds further value to the spacetime metric solutions obtained from relativity. Upon asserting physical viability of the field equations obtained, it is of interest to consider pressure anisotropy as this allows for a nonvanishing tangential pressure at the boundary of the star and this can be linked to a modification of the surface tension. The tangential pressure has been found in previous studies to grow monotonically from zero at the star center to a value in the range of $20 \sim 50\ \mathrm{MeV/fm^3}$ for quark star models with masses in the range $1.29M_\odot$ to $1.85M_\odot$ [17].

An equation of state (EoS) is also frequently used in promoting physical viability and setting certain parameters which arise during the determination of the metric potentials [16,18,19]. Linear, quadratic, polytropic, and van der Waal's equations of state have been used previously to model compact stars [20,21] ranging from white dwarfs to highly dense neutron stars and quark stars. In the case of quark or strange-quark stars, the MIT bag model of QCD, which allows for a confinement pressure in addition to the degeneracy pressure, makes use of a linear EoS of the form $p = \frac{1}{3}(\rho - 4B)$ [22]. In this form, the MIT bag constant $4B$ is linked to a surface density [23]. A study of compact objects using the Vaidya-Tikekar ansatz [24], suitable for so-called superdense stars, has shown a linear relationship between the energy density and the isotropic pressure, so a linear equation of state is generally a good approximation for very dense, compact objects such as strange stars [25]. Further improvements can be made to take into account the deconfinement of quarks at high density, and this might require a departure from linearity. In our work, we allow the pressure to be anisotropic in order to study its affect on the surface tension, and departure from a linear EoS might highlight new physical properties arising from the inclusion of strange quark mass and QCD gap energies due to quark interactions. Rocha *et al.* [26,27] have recently done a study on compact stars composed of CFL quark matter where they used an equation of state of the form $p_r = \alpha\rho + \beta\rho^{1/2} - \gamma$. In the case $\beta = 0$, this reduces to the MIT bag model EoS. Thirukkanesh *et al.* [28] carried out a comparison between compact objects obeying the MIT bag model and the CFL equation of state in isotropic coordinates. Two new classes of exact solutions obeying the CFL equation of state were obtained. These models were shown to be physically viable in terms of a description of compact objects in general relativity.

In this paper, we employ the CFL equation of state to investigate the effect of the bag parameter and the QCD gap energy on the surface tension of compact objects such as neutron stars and strange-quark stars. In Sec. II, we present the line element and the matter tensor describing the geometry and matter content of the compact object. We also introduce the CFL equation of state. The equation governing the surface tension for an anisotropic fluid sphere is derived in Sec. III. A rigourous analysis of our results is carried out in Sec. IV, which is followed by a discussion of our findings in Sec. V. We conclude with an overview in Sec. VI.

II. FIELD EQUATIONS

The line element for a static spherical object in the standard form is given by

$$ds^2 = -e^{\nu}c^2dt^2 + e^{\lambda}dr^2 + r^2(d\theta^2 + \sin^2\theta d\phi^2), \quad (1)$$

where $\nu(r)$ and $\lambda(r)$ are the gravitational potentials. The energy-momentum tensor for an anisotropic star may be written as

$$T_{ij} = (\rho c^2 + p_r)u_i u_j + p_r g_{ij} + (p_r - p_t)n_i n_j, \quad (2)$$

where ρ is the energy density; p_r and p_t are the radial and tangential pressures, respectively; u_i is the fluid four-velocity; and n_i is a radially directed unit spacelike vector.

Einstein's field equations are then given by

$$\frac{8\pi G}{c^4}\rho = \frac{(1 - e^{-\lambda})}{r^2} + \frac{\lambda' e^{-\lambda}}{r}, \quad (3)$$

$$\frac{8\pi G}{c^4}p_r = \frac{\nu' e^{-\lambda}}{r} - \frac{(1 - e^{-\lambda})}{r^2}, \quad (4)$$

$$\frac{8\pi G}{c^4}p_t = \frac{e^{-\lambda}}{4}\left(2\nu'' + (\nu')^2 - \lambda'\nu' + \frac{2\nu'}{r} - \frac{2\lambda'}{r}\right), \quad (5)$$

which have been used previously by researchers [18]. An equation of state which is suitable for describing strange quark matter in the CFL phase [26,27] is given by

$$p_r = \frac{1}{3}\rho + \frac{2\eta}{\pi}\rho^{1/2} - \left(\frac{3\eta^2}{\pi^2} + \frac{4}{3}B\right), \quad (6)$$

where

$$\eta = -\frac{m_s^2}{6} + \frac{2\Delta^2}{3}. \quad (7)$$

It incorporates the MIT bag constant B and, in addition, the strange quark mass m_s and a QCD gap energy Δ which accounts for quark interactions. These parameters are needed in calculating the chemical potential [29], which is given by

$$\mu = \left(-\eta + \sqrt{\eta^2 + \frac{4}{9}\pi^2(\bar{\rho} - \bar{B})}\right)^{1/2}, \quad (8)$$

where $\bar{B}$ and $\bar{\rho}$ are the MIT bag constant and energy density, respectively, as expressed in terms of standard particle physics units of $[\mathrm{MeV}^4]$ with the conversions being $B = \bar{B}/(\hbar c)^3$ and $\rho = \bar{\rho}/(\hbar c)^3$.

It is noted that the chemical potential should preferably be greater than 300 MeV [29], and this serves as a guide for choosing suitable values for m_s and Δ. The baryon number density may then be calculated from

$$n_B = \frac{\mu^3}{\pi^2} - \frac{m_s^2 \mu}{2\pi^2} + \frac{2}{\pi^2}\Delta^2\mu \tag{9}$$

which gives the density of baryons at the surface as required. It is worth comparing the baryon number density to the well-documented number density at nuclear saturation ($0.16\ \mathrm{fm}^{-3}$) [30], often used for normalization in plots.

III. SURFACE TENSION OF ANISOTROPIC FLUIDS

Bagchi *et al.* [6], have shown that compact objects composed of u, d, s quarks should have a greater surface tension than that of neutron stars. In calculating the surface tension, it is assumed that the star is a large spherical ball composed of strange matter which is self-bound and nonrotating. The excess pressure on the surface of the star can then be expressed as

$$|\Delta p|_{r=R} = \frac{2\sigma}{R}, \tag{10}$$

where σ is the surface tension of the star and R is the radius of curvature, corresponding to the surface boundary. Although this is an application of the classical Young-Laplace equation and thus perhaps simplistic, it has been used previously in calculating the surface tension of strange stars [6,18,31]. Recently, it has been shown that a relativistic correction could further increase the surface tension [32] whereby values of σ obtained via the Young-Laplace method could be augmented by a factor $(1 - 2M/R)^{-1/2}$, M being the geometrized mass of the star. This is open for further investigation and comparison with more sophisticated methods of computing surface tension such as variation of the chemical potential and Gibbs free energy.

At the surface of the star, the excess pressure can be related to the pressure gradient, given by

$$|\Delta p|_{r=R} = r_n \left|\frac{dp}{dr}\right|_{r=R}, \tag{11}$$

where r_n is the radius of the quark particle. The radius is given by

$$r_n = (1/\pi n_B)^{1/3}, \tag{12}$$

where n_B is the baryon number density. Owing to the highly compact nature of strange stars, a relativistic treatment is necessary in finding internal configurations and the various physical parameters. For a given EoS, one can use the generalized Tolman-Oppenheimer-Volkoff (TOV) equation [33] in which pressure anisotropy may be included, namely

$$\frac{dp}{dr} = -\frac{G(\rho + p)[\frac{m(r)}{c^2 r} + \frac{4\pi r^2 p}{c^4}]}{r(1 - \frac{2Gm(r)}{c^2 r})} + \frac{2}{r}(p_t - p_r) \tag{13}$$

as done previously in surface tension studies [18].

The TOV equations may also be written in the form

$$-\frac{M_G(\rho + p_r)}{r^2} e^{\frac{\lambda-\nu}{2}} - \frac{dp_r}{dr} + \frac{2}{r}(p_t - p_r) = 0, \tag{14}$$

where $M_G = M_G(r)$ is the Tolman-Whittakar gravitational mass inside a sphere of radius r [34]. This effective gravitational mass is given by

$$M_G(r) = \frac{1}{2} r^2 e^{\frac{\nu-\lambda}{2}} \nu' \tag{15}$$

so that (13) is regained upon applying the Schwarzschild metric. The form of (14) is useful in testing for equilibrium whereby the components of force are given as

$$\begin{aligned} F_h &= -\frac{dp_r}{dr} \\ F_g &= -\frac{M_G(\rho + p_r)}{r^2} e^{\frac{\lambda-\nu}{2}} \\ F_a &= \frac{2}{r}(p_t - p_r), \end{aligned} \tag{16}$$

where F_h, F_g, and F_a denote hydrostatic, gravitational, and anisotropic forces, respectively.

Substituting (3) and (4) into (6), we obtain

$$\nu' = \frac{1}{3}\left[\frac{4}{r}(e^\lambda - 1) + \lambda' - 4re^\lambda \frac{G}{c^4}\left(8\pi B + \frac{18}{\pi}\eta^2 - \sqrt{\frac{18}{\pi}}\eta \times \sqrt{\frac{c^4}{Gr^2} e^{-\lambda}(r\lambda' + e^\lambda - 1)}\right)\right]. \tag{17}$$

We then make use of the Finch-Skea ansatz [35] and set the metric potential

$$e^\lambda = 1 + \frac{r^2}{\mathcal{R}^2}, \tag{18}$$

where $\mathcal{R}$ is a scaling parameter related to the curvature. The spacetime geometry of Finch and Skea has recently been used by Sharma *et al.* [36] for obtaining closed-form solutions for a spherically symmetric anisotropic matter distribution. Furthermore, the suitability of the Finch-Skea model for describing strange stars was also noted.

Substituting our expression for ν' and evaluating at the surface boundary $[p_r(r=R)=0]$, the TOV equation becomes

$$\left.\frac{dp_r}{dr}\right|_{r=R} = \frac{2}{R}p_t(R) - \frac{\rho(R)}{3R}\left[\frac{1}{1+(\mathcal{R}/R)^2} + \frac{2}{(\mathcal{R}/R)^2} - \frac{2GR^2}{c^4}\left(1+\frac{R^2}{\mathcal{R}^2}\right)\left(8\pi B + \frac{3\eta}{\pi}\left(6\eta - \sqrt{\frac{2\pi c^4(1+3(\mathcal{R}/R)^2)}{GR^2(1+(\mathcal{R}/R)^2)^2}}\right)\right)\right], \tag{19}$$

where $p_t(R)$ and $\rho(R)$ are the tangential pressure and the energy density, respectively, evaluated at the surface. As seen here, pressure anisotropy features prominently in our work. In a recent study [14], Herrera has remarked on the importance of pressure anisotropy $(p_t > p_r)$ to help explain the possibility for more compact objects in contrast to models which are isotropic. In this regard, pressure anisotropy is seen to be a relativistic effect and, in essence, an intrinsic property of relativistic hydrodynamics.

The expression for surface tension is now computed as

$$\sigma = \left| r_n p_t(R) - \frac{r_n\rho(R)}{6}\left[\frac{1}{1+(\mathcal{R}/R)^2} + \frac{2}{(\mathcal{R}/R)^2} - \frac{2GR^2}{c^4}\left(1+\frac{R^2}{\mathcal{R}^2}\right)\left(8\pi B + \frac{3\eta}{\pi}\left(6\eta - \sqrt{\frac{2\pi c^4(1+3(\mathcal{R}/R)^2)}{GR^2(1+(\mathcal{R}/R)^2)^2}}\right)\right)\right]\right|, \tag{20}$$

where the radius of the quark particle, r_n, is determined from the baryon number density (9) as given by (12). The surface tension of strange stars is still uncertain. Early work by Heiselberg [30] suggested that $\sigma > 70\ \mathrm{MeV/fm^2}$ for a transition from nucleon to quark matter; however, lower values of a few $\mathrm{MeV/fm^2}$ have been found sufficient in some cases [31]. These are often set as critical values, associated with the stability of strangelets of the order of tens of femtometers in size. A much larger compact object might require significantly larger energies for maintaining the surface-vacuum interface.

IV. PHYSICAL ANALYSIS

We set the Finch-Skea parameter $\mathcal{R} = 9.50$ km which provides a suitable mass-radius relationship for modeling potential strange-star candidates as shown in Fig. 1. In particular, a star with a central core density of $1.78 \times 10^{15}\ \mathrm{g/cm^3}$ and a surface density of $4.10 \times 10^{14}\ \mathrm{g/cm^3}$ is calculated for a radius of $R = 11.9$ km. This is in agreement with $\rho(R) = 4B/c^2$ for the simplest bag model of

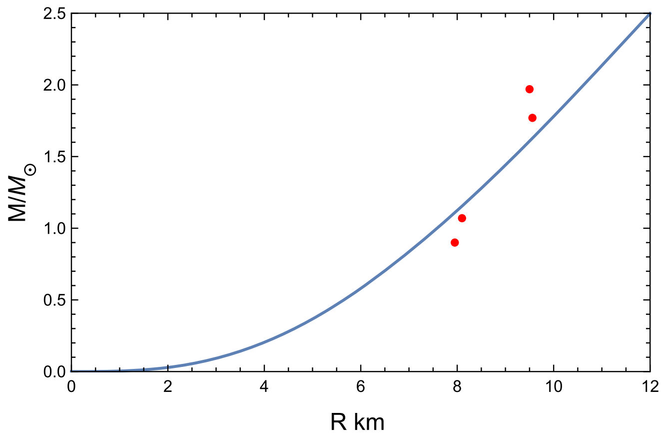

FIG. 1. Mass-radius relationship for Finch-Skea parameter $\mathcal{R} = 9.50$ km. Points denote strange-star candidates given in Table II.

massless, noninteracting quarks with the MIT bag constant set at $57.5\ \mathrm{MeV/fm^3}$ [37]. It is also noted that the core density is less than 5 times the surface density, consistent with highly compact quark matter. This is in contrast with neutron stars where the core density is typically expected to be 2 to 3 orders of magnitude greater than that at the surface [38].

We then augment this model to include the strange quark mass and the QCD gap energy parameter, Δ. Since pressure anisotropy is of particular importance in our study, we first plot the pressure profiles and the anisotropy parameter $\delta = p_t - p_r$ as shown in Figs. 2 and 3, respectively. The shape of the curves and the surface tangential pressure $(p_t(R) = \delta(R))$ calculated compare well with other studies [17,23,36]. By lowering the Finch-Skea parameter, one can enhance the anisotropy so that larger surface tangential pressures are obtained, but this results in masses and radii which are larger and uncharacteristic of neutron stars and proposed strange star candidates.

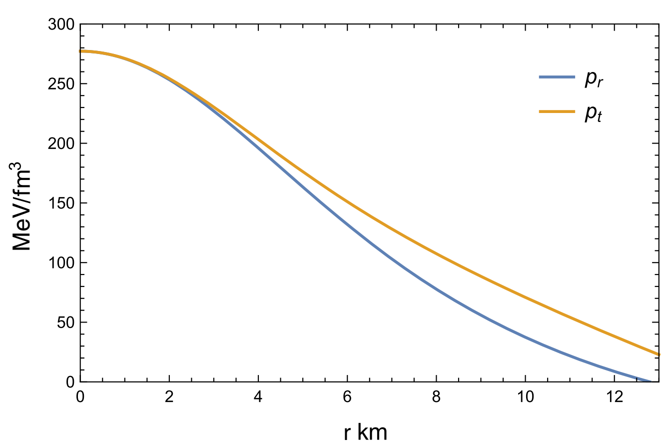

FIG. 2. Radial and tangential pressure profiles for quark energy parameters $\Delta = 100$ MeV and $m_s = 150$ MeV with bag constant set at $57.5\ \mathrm{MeV/fm^3}$.

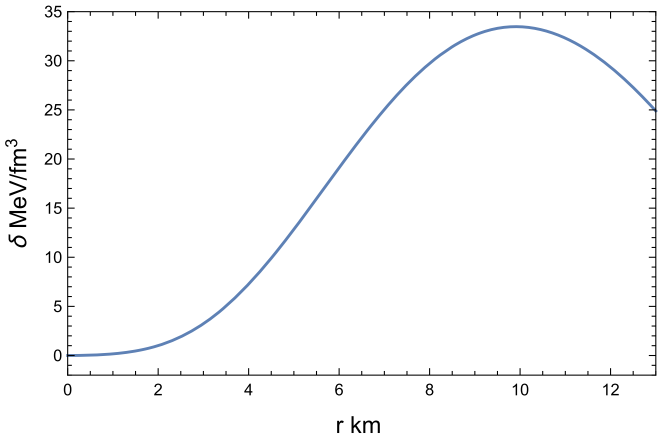

FIG. 3. Anisotropy parameter profile for quark energy parameters $\Delta = 100$ MeV and $m_s = 150$ MeV with bag constant set at 57.5 $\mathrm{MeV/fm^3}$.

By allowing the bag constant and quark parameters to vary, and using the boundary condition $p_r(r = R) = 0$, we obtain the model parameters listed in Table I. In Table II, we list observed physical parameters of candidate strange stars for comparison.

Similar values for the MIT bag constant B, strange quark mass m_s and gap energy Δ have been used by Rocha *et al.* [26]. Equation (20) is then used to plot the surface tension with respect to the tangential surface pressure for different values of the bag constant and quark energies. These are shown in Figs. 6–8. The linear dependence of the surface tension on tangential pressure, as also shown by Sharma and Maharaj [18], is a consequence of the form of the generalized TOV equation used. The TOV equation could be modified further to include charge distributions and magnetic fields, and higher order theories of gravity could also introduce additional nonlinear terms involving pressure and energy density. Since it is a necessary physical constraint that the pressure gradient within the stellar interior remain negative, we conclude that there are limiting values of the surface tangential pressure beyond which the system is not physically viable. Our calculated values of surface tangential pressure do not approach this region. The plots given in Figs. 6–8 could be extrapolated to the low critical values of surface tension obtained via studies on strangelets [31], and this could serve as an upper bound for physically viable values of tangential pressure and anisotropy.

TABLE II. Observed physical parameters of some strange star candidates [39].

Strange star candidate	$M/M_\odot$	Radius (km)
Her X-1	1.07 ± 0.36	8.1 ± 0.41
PSR J1614-2230	1.97 ± 0.04	9.5
Vela X-1	1.77 ± 0.08	9.56 ± 0.08
SAX J1808.4-3658	0.9 ± 0.3	7.95

V. DISCUSSION

Our model parameters of mass and star radius given in Table I are comparable with observed data given in Table II. This is clearly seen in the mass-radius relationship given in Fig. 1. Values of masses and radii that are closest to those of typical strange star candidates appear to be favored by the higher bag constant of $B = 80\ \mathrm{MeV/fm^3}$. Figure 2 shows the variation of the radial and tangential pressures at each interior point of the star. The radial and tangential stresses decrease monotonically outward with the tangential pressure becoming more dominant in the surface layers of the stellar configuration. The variation of the pressure anisotropy parameter with radial coordinate is given in Fig. 3. This parameter is positive throughout the stellar interior, giving rise to a repulsive force. This force helps stabilize the configuration with respect to the gravitational force. Figure 4 shows the equation of state parameter in both the radial and tangential directions. These functions are continuous and well behaved throughout the stellar interior, and the effect of the anisotropy is clearly seen, providing for a stiffer matter content within the outer stellar region. The forces associated with the TOV equation are shown in Fig. 5. It is clear that the sum of the three forces is zero ($F_\Sigma = F_h + F_g + F_a = 0$) at each interior point of the configuration, thus indicating a state of equilibrium.

TABLE I. Model parameters.

Model No.	$M/M_\odot$	R (km)	B $(\mathrm{MeV/fm^3})$	Δ (MeV)	m_s (MeV)	n_B $(\mathrm{fm^{-3}})$	$p_t(R)$ $(\mathrm{MeV/fm^3})$	σ $(\mathrm{MeV/fm^2})$
1	2.79	12.8	57.5	100	150	0.293	25.9	80.6
2	2.27	11.4	70	100	150	0.338	13.8	84.9
3	1.94	10.5	80	100	150	0.373	5.0	87.1
4	2.47	11.9	57.5	0	0	0.278	23.1	70.5
5	2.00	10.6	70	0	0	0.322	11.1	76.0
6	1.70	9.75	80	0	0	0.356	2.6	78.7
7	2.23	11.3	57.5	50	150	0.266	20.6	64.0
8	1.80	10.0	70	50	150	0.310	8.9	70.0
9	1.52	9.24	80	50	150	0.343	0.6	73.2

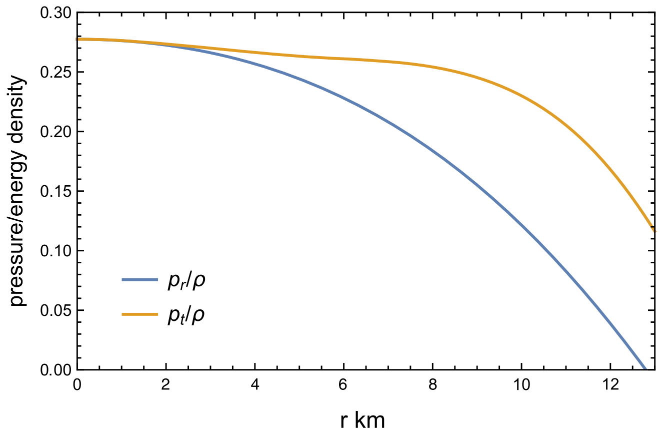

FIG. 4. Equation of state parameter profile for quark energy parameters $\Delta = 100$ MeV and $m_s = 150$ MeV with bag constant set at 57.5 MeV/fm^3.

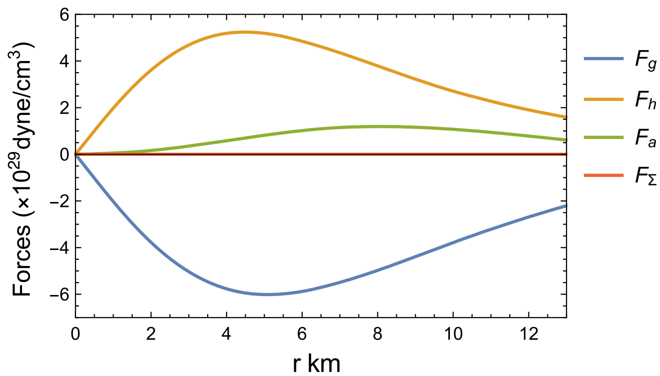

FIG. 5. Decomposition of the TOV equation into force components for quark energy parameters $\Delta = 100$ MeV and $m_s = 150$ MeV with bag constant set at 57.5 MeV/fm^3.

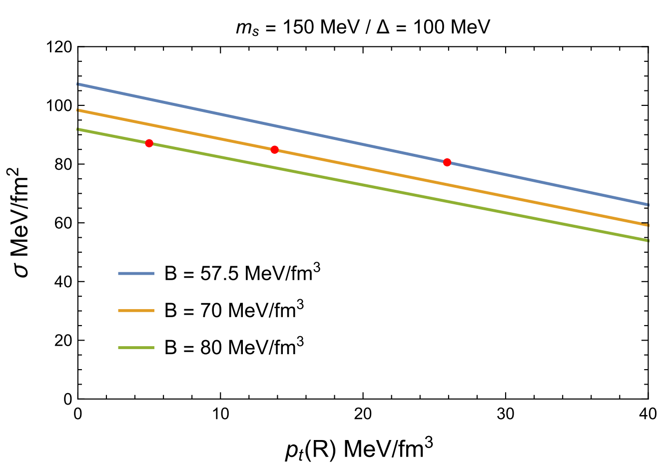

FIG. 6. Surface tension-tangential pressure relationship for quark energy parameters $\Delta = 100$ MeV and $m_s = 150$ MeV. Points denote model parameters from Table I.

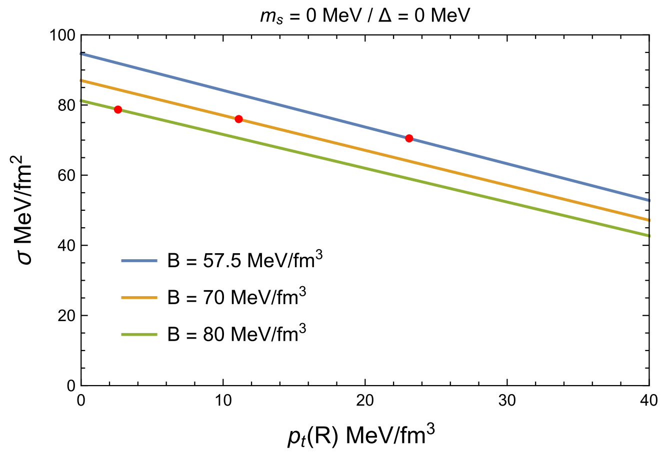

FIG. 7. Surface tension-tangential pressure relationship for quark energy parameters $\Delta = m_s = 0$ MeV. Points denote model parameters from Table I.

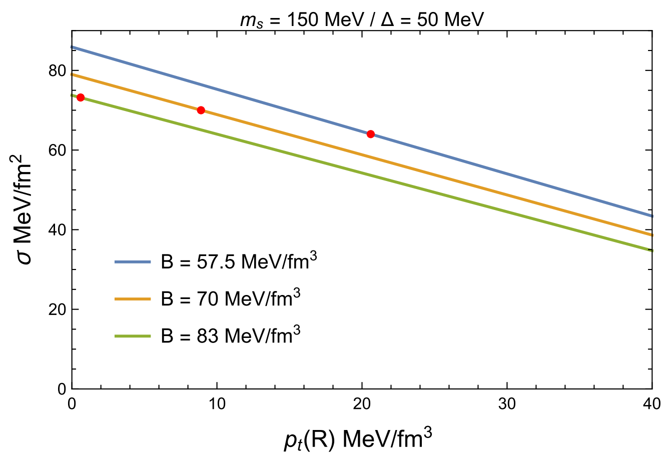

FIG. 8. Surface tension-tangential pressure relationship for quark energy parameters $\Delta = 50$ MeV and $m_s = 150$ MeV. Points denote model parameters from Table I.

Figures 6–8 may be compared with those obtained by Sharma and Maharaj [18]. Both the surface tensions and the tangential pressures are generally lower as might be expected for stars with lower densities and larger radii as compared with the two more highly compact systems studied by Sharma and Maharaj. We note that an increase in the vacuum energy (larger values for the bag constant) promotes systems with lower tangential pressures and surface tensions. Although the use of the Finch-Skea model in our study produced relatively low values of tangential pressure, it is noted that other models with gravitational potentials more suited to superdense compact objects could result in higher surface tangential pressures. This could significantly reduce the resulting pressure gradient to levels which would provide smaller surface tensions. However, our tangential pressures compare well with pressures obtained from other studies on CFL equations of state

[28] and, in addition, to induced surface tension equations of state [5]. According to our study, low values of surface tension are achievable for tangential pressures greater than 80 $\mathrm{MeV/fm^3}$ for the typical quark energy parameters $m_s = 150$ MeV and $\Delta = 100$ MeV.

Lower gap energies seem to favor lower surface tensions, and this could be important near critical values for quark matter to hadronic matter transitions. For noninteracting and massless quarks, the 70 $\mathrm{MeV/fm^2}$ critical value originally proposed by Heiselberg [30] is attainable from our models, apart from model number in Table I. It is expected that the gap energy should be at least 100 MeV [30,40] for massive strange quarks in the superconducting CFL phase and model numbers 7 and 9 are somewhat indicative of this. In our study, we did not exceed $B = 80\ \mathrm{MeV/fm^3}$ as this resulted in unreasonable behavior in the anisotropy parameter with vanishing tangential pressures. Values such as $B = 115\ \mathrm{MeV/fm^3}$ have been used by Rocha *et al.* [26] in CFL equation of state studies; however, this resulted in unreasonably low masses and radii in our gravitational model.

VI. CONCLUSION

In this work, we calculated and studied the surface tension of compact objects as mediated by a color-flavor-locked equation of state. Our results generalize the earlier work of Sharma and Maharaj [18] in which they utilized a linear EoS, with the necessity of allowing for pressure anisotropy being reaffirmed. The gravitational behavior of our model was determined by employing the Finch and Skea ansatz together with the CFL EoS. It is noted that the Finch and Skea ansatz is very effective in providing computed physical parameters which are realistic and comparable to other studies of highly compact objects. More sophisticated gravitational potential formulations, specific to superdense compact objects, could be applied in future studies. A formula for the surface tension was derived by utilizing the generalized TOV equation incorporating pressure anisotropy and the CFL EoS. We believe that this is the first attempt at relating the surface tension of a compact object in general relativity to the MIT bag constant and the QCD gap energy parameter. Our findings indicate that configurations with lower surface tension can be achieved for smaller QCD gap energies and vacuum energies. The surface tensions computed for our models are in the range $\sigma = 60 - 90\ \mathrm{MeV/fm^2}$, which is comparable with other studies. Since these values are significantly larger than the critical values of a few $\mathrm{MeV/fm^2}$ found for strange quark matter in the form of strangelets, we conclude that our model likely excludes the possibility of exotic surfaces such as one in which strangelets are bound within a crystalline or quasicrystalline setting. Our model thus appears to be more compatible with a homogeneous surface, which could be fluidic in nature. Previous studies in which surface tensions of about $4 \sim 10\ \mathrm{MeV/fm^2}$ were calculated [31]; also note that the surface tension would certainly be larger if the interface boundaries had finite thicknesses rather than the infinitely sharp interfaces assumed in QCD calculations. Thus, it is likely that $\sigma \gg \sigma_{\mathrm{crit}}$ in order for larger strangelets to remain stable should the surface of a quark star be composed of these. The importance of pressure anisotropy in our model was shown. Lower surface tensions might be obtained by using gravitational models, which further enhance pressure anisotropy, but we have also shown that the surface tangential pressure could have limiting values if our surface tension plots are extrapolated. Finally, in terms of the use of the CFL EoS, our results support observations made by Thirukkanesh *et al.* [28] that the linear EoS is a good approximation to the CFL EoS for particular combinations of the QCD gap energy and the MIT bag constant.

ACKNOWLEDGMENTS

R. B. and M. G. acknowledge financial support from the office of the Deputy Vice-Chancellor: Research and Innovation at the Durban University of Technology. We also thank the referees for their comments.

[1] M. Dey, I. Bombaci, J. Dey, S. Ray, and B. C. Samanta, Phys. Lett. B **438**, 123 (1998).

[2] E. Witten, Phys. Rev. D **30**, 272 (1984).

[3] E. Farhi and R. Jaffe, Phys. Rev. D **30**, 2379 (1984).

[4] F. Weber, Prog. Part. Nucl. Phys. **54**, 193 (2005).

[5] V. V. Sagun, I. Lopes, and A. I. Ivanytskyi, Astrophys. J. **871**, 157 (2019).

[6] M. Bagchi, M. Sinha, M. Dey, J. Dey, and S. Bhowmick, Astron. Astrophys. **440**, L33 (2005).

[7] M. G. Alford and D. A. Eby, Phys. Rev. C **78**, 045802 (2008).

[8] F. Gao and Y.-X. Liu, Phys. Rev. D **94**, 094030 (2016).

[9] X.-J. Wen, J.-Y. Li, J.-Q. Liang, and G.-X. Peng, Phys. Rev. C **82**, 025809 (2010).

[10] G. Lugones, A. Grunfeld, and M. A. Ajmi, Phys. Rev. C **88**, 045803 (2013).

[11] C.-J. Xia, G.-X. Peng, T.-T. Sun, W.-L. Guo, D.-H. Lu, and P. Jaikumar, Phys. Rev. D **98**, 034031 (2018).

[12] R. L. Bowers and E. P. T. Liang, Astrophys. J. **188**, 657 (1974).
[13] L. Herrera, G. L. Denmat, and N. O. Santos, Gen. Relativ. Gravit. **44**, 1143 (2012).
[14] L. Herrera, Phys. Rev. D **101**, 104024 (2020).
[15] M. R. S. Delgaty and K. Lake, Comput. Phys. Commun. **115**, 395 (1998).
[16] P. M. Takisa, S. Ray, and S. D. Maharaj, Astrophys. Space Sci. **350**, 733 (2014).
[17] F. Tello-Ortiz, M. Malaver, A. Rincon, and Y. Gomez-Leyton, Eur. Phys. J. C **80**, 371 (2020).
[18] R. Sharma and S. D. Maharaj, Mon. Not. R. Astron. Soc. **375**, 1265 (2007).
[19] R. P. Pant, S. Gedela, R. K. Bisht, and N. Pant, Eur. Phys. J. C **79**, 602 (2019).
[20] B. P. Brassel, R. Goswami, and S. D. Maharaj, Phys. Rev. D **95**, 124051 (2017).
[21] F. C. Ragel and S. Thirukkanesh, Eur. Phys. J. C **79**, 306 (2019).
[22] S. Biswas, D. Shee, S. Ray, F. Rahaman, and B. K. Guha, Ann. Phys. (Amsterdam) **409**, 167905 (2019).
[23] M. Govender and S. Thirukkanesh, Astrophys. Space Sci. **358**, 39 (2015).
[24] P. Bhar, Eur. Phys. J. C **75**, 123 (2015).
[25] J. L. Zdunik, Astron. Astrophys. **359**, 311 (2000), arXiv: astro-ph/0004375.
[26] L. Rocha, A. Bernardo, M. G. B. D. Avellar, and J. E. Horvath, Int. J. Mod. Phys. D **29**, 2050044 (2020).
[27] L. S. Rocha, A. Bernardo, M. G. B. de Avellar, and J. E. Horvath, Astron. Nachr. **340**, 180 (2019).
[28] S. Thirukkanesh, A. Kaisavelu, and M. Govender, Eur. Phys. J. C **80**, 214 (2020).
[29] G. Lugones and J. E. Horvath, Phys. Rev. D **66**, 074017 (2002).
[30] H. Heiselberg, arXiv:hep-ph/9501359v1.
[31] M. G. Alford, K. Rajagopal, S. Reddy, and A. W. Steiner, Phys. Rev. D **73**, 114016 (2006).
[32] H. Culetu, arXiv:gr-qc/2004.13010.
[33] R. C. Tolman, Phys. Rev. **55**, 364 (1939).
[34] A. Aziz, S. Ray, F. Rahaman, M. Khlopov, and B. K. Guha, Int. J. Mod. Phys. D **28**, 1941006 (2019).
[35] M. R. Finch and J. E. F. Skea, Classical Quantum Gravity **6**, 467 (1989).
[36] R. Sharma, S. Das, and S. Thirukkanesh, Astrophys. Space Sci. **362**, 232 (2017).
[37] P. Haensel, A. Y. Potekhin, and D. G. Yakovlev, in *Neutron Stars 1* (Springer, New York, 2007), Chap. 8.
[38] A. L. Watts, N. Andersson, D. Chakrabarty, M. Feroci, K. Hebeler, G. Israel, F. K. Lamb, M. C. Miller, S. Morsink, F. Ozel, A. Patruno, J. Poutanen, D. Psaltis, A. Schwenk, A. W. Steiner, L. Stella, L. Tolos, and M. van der Klis, Rev. Mod. Phys. **88**, 021001 (2016).
[39] T. Gangopadhyay, S. Ray, X.-D. Li, J. Dey, and M. Dey, Mon. Not. R. Astron. Soc. **431**, 3216 (2013).
[40] K. Rajagopal and F. Wilczek, Phys. Rev. Lett. **86**, 3492 (2001).